Microporous and Mesoporous Materials 201 (2015) 17–23

Contents lists available at ScienceDirect

Microporous and Mesoporous Materials

journal homepage: www.elsevier.com/locate/micromeso

Acid properties and catalysis of USY zeolite with different extra-framework aluminum concentration

Xin Pu, Nai-wang Liu, Li Shi *

The State Key Laboratory of Chemical Engineering, East China University of Science and Technology, Shanghai 200237, PR China

ARTICLE INFO

Article history:
Received 26 June 2014
Received in revised form 20 August 2014
Accepted 26 August 2014
Available online 6 September 2014

Keywords:
USY
Acid property
Dealumination
X-ray diffraction
Extra framework aluminum

ABSTRACT

USY zeolite was treated by the citric acid. The properties and catalysis of the USY zeolite were studied. The X-ray diffraction has been used to identify and quantify extra framework aluminum (EFAL) in USY zeolite by EFAL extraction using citric acid. The acid character changed depending on the EFAL concentration. The Lewis acid sites can be obtained from the Si/Al ratio. The removing of trace olefins was carried out over kinds USY zeolites with different amount of EFAL. The catalytic performance was correlated with the Lewis acid sites of USY.

1. Introduction

Aromatics hydrocarbon such as benzene, toluene, xylene and ethyl benzene (BTX) are obtained from reforming and cracking processes in the petrochemical enterprises. The conversion of naphtha into BTX stream is always accompanied by the formation of non-aromatic olefins such as hexene and styrene [1–2]. These olefins can poison the adsorbent which is used to separate para-xylene (PX) from aromatics. In order to protect the adsorbent, the bromine index which is an indicator of the presence of olefinic bonds is required to be less than 20 mg Br/100 g. Therefore, these contaminants must be removed before aromatic streams are sent to the petrochemical processes. It has been approved that these harmful impurities can be removed by acid-catalyzed alkylation of the appropriate aromatics [3–4]. In commercial plants, the purification process uses the clay treating [5] or the modified clay treatment. But, both of the two methods pose problems such as limited lifetime, pollution and non-reused. Pressure from legislative and environmental bodies together with a growing awareness within the chemical industry has led to a search for new eco-friendly products and processes to replace polluting reactions.

USY zeolite is one of the most important zeolites applied in industry for petroleum processes, which is the ultrastable counterpart of Y zeolite, and was obtained by steaming treatment of Y zeolite [6–7]. To obtain highly siliceous zeolite Y, it is necessary to have a post-synthesis treatment (dealumination), in which the Al atom is expelled from the zeolite lattice. As a result, extra-framework Al species is formed. Dealumination can be accomplished by thermal or hydrothermal treatments, chemical treatments and acids leaching [8–10]. The resulting material, USY zeolites, being modified in the framework Si/Al ratio, structure and acidity, usually exhibit improved reactivity, selectivity and coking behavior for a catalytic reaction, which is of great interest to the petroleum industry [11]. It has been suggested that the amount of extra-framework Al species, formed during the process of dealumination, is one of the key factors that influence significantly catalytic activity [12].

Citric acid, as an acid and a chelating agent for metal ion, is effective for the extraction of aluminum from zeolite [11]. The USY zeolite will have a rich acid strength after treating by citric acid. The modified process can change the distribution of the acid in the zeolite. The amount of Lewis (L) acid was increased and the amount of Brønsted (B) acid was decreased. Here the conditions for treatment of USY zeolites by citric acid and the influence of acid treatment on the properties of obtained USY zeolites were systematically studied. Furthermore, removing of trace olefins from aromatics was explored by using the obtained USY zeolite as catalyst.

2. Experimental section

2.1. Materials

USY powder was purchased from XinNian Petrochemical Additives Company (China) and was referred as USY-parent. Citric acid

* Corresponding author. Tel.: +86 021 64252274.
E-mail address: yyshi@ecust.edu.cn (L. Shi).

http://dx.doi.org/10.1016/j.micromeso.2014.08.056
1387-1811/

(AR, 99.8%) was purchased from Sinopharm Chemical Reagent Company, China. Experimental raw materials were aromatic intermediate products without the clay treatment, which were obtained from industrial reforming units of Sinopec Zhenhai Refining & Chemical Company. The main components were C8–C10 which can be seen in Table 1.

2.2. Preparation of the USY zeolites

Modified USY was prepared by acid leaching method. In a typical procedure, ten gram of USY zeolites and the solution of citric acid (250 ml) were placed into a three-necked flask equipped with a reflux condenser. After treatment at 363 K for a certain time under stirring, the sample was filtered, washed with deionized water, dried overnight at 493 K.

A series of modified USY zeolites were prepared by the treatment of USY with an acid solution (0.1, 0.2 and 0.3 mol L^{-1}) for 4 h. Codes *f* samples reflect their treatment conditions. If the sample was leached by 0.1 mol L^{-1} citric acid, it is denoted by USY-0.1, while USY-0.3 means that the USY was treated with 0.3 mol L^{-1} acid for 4 h.

2.3. Characterization of USY zeolites

X-ray diffraction (XRD) of the representative samples (before the kneading) were performance on a Rigaku-3014 diffractometer with a monochromator using Cu Kα (λ = 0.154 nm) radiation. The diffractograms were recorded in the 2θ range 10–80° in steps of 0.04° with a scan rate of 2° per min. The crystallinities of the samples were calculated according to the intensity of the peaks at 2θ of 11.9°, 15.7°, 18.7°, 20.4°, 23.7°, 27.1° and 31.4°. The nitrogen adsorption of the samples (before the kneading) were performed on a Micromeritics 2010 analyzer at liquid nitrogen temperature (77.3 K) and the samples were degassed at 673 K for 4 h prior to adsorption analysis. The in situ IR spectra of OH groups and pyridine adsorption were run on a Nicolet 6700 Fourier transform IR spectrometer. The surface acidity was investigated by the adsorption of pyridine on the solid surface of samples. FTIR measurements were carried out using pyridine as probe molecule. The Fourier transform infrared spectra was collected with a combined reactor-spectrometer system using a low-volume in situ cell with water-cooled KBr window (see Fig. 1).

For all experiments, 16.5–16.9 mg of finely ground catalyst was pressed into self-supporting wafers with a diameter of 10 mm. The wafer loaded into the cell was pretreated at 653 K in vacuum conditions for 2 h and cool down to 353 K for pyridine adsorption. The physisorbed pyridine was eliminated at 473 K. The total concentrations of Brønsted and Lewis sites able to retain pyridine at 473 K were determined using the absorbance surfaces of the corresponding bands at 1540 and 1450 cm^{-1}, respectively [13–14]. Then the sample was subjected to the thermal desorption at 723 K followed by the IR measurement. Through the FTIR spectroscopy, the strong acid sites can be monitored. The difference represents the weak acid sites. The quantification method for Lewis acidic site and Brønsted acidic site was based on Lambert–Beer law: $A = \xi \cdot C \cdot d$, where A is absorbance, C is the sample concentration, ξ is extinction coefficient and d is sample thickness. Surface acid contents of adsorbents for Lewis acid and Brønsted acid were calculated by using empirical formulas which are obtained from the relevant experiments.

$$C_L(\text{mol g}^{-1}) = 3.73 \times 10^{-4} \cdot A_L \quad (1)$$

$$C_B(\text{mol g}^{-1}) = 9.90 \times 10^{-4} \cdot A_B \quad (2)$$

where C_L and C_B are respectively Lewis acid contents and Brønsted acid contents (mol g^{-1}) , A_L and A_B are respectively peak areas in 1450 cm^{-1} (denoted as L acid sites) and in 1540 cm^{-1} (denoted as B acid sites).

Table 1
Composition of the aromatics of Sinopec Zhenhai Refining & Chemical Company.

Raw material (with Bromine Index of 1120) w%					
Toluene	Ethyl benzene	Xylene	C_9 aromatics	C_{10} aromatics	Others
0.238	7.885	52.207	32.622	6.81	0.238

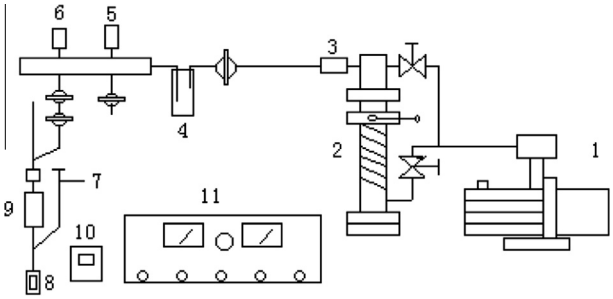

Fig. 1. In situ FTIR reactor system. (1) Rotary vane vacuum pumps. (2) High vacuum oil diffuse pump. (3) Antihunting device. (4) Buffer unit. (5) Vacuum gauge. (6) Thermocouple well. (7) Pyridine entrance. (8) Infrared transmission windows. (9) Heater coil. (10) Temperature controller and solid state relays. (11) Composite vacuum table.

2.4. Micro-activity test evaluation

The modified sample was powdered, and mixed with alumina (the weight ratio of zeolite/alumina was 4) to prepare modified zeolite catalyst, kneaded with the proper amount of a 10% nitric acid solution, and then squeezed into the form of strips. The moisture was removed in an oven, in an air atmosphere at 393 K for 6 h. Then, the catalyst was activated at 823 K for 6 h. After cooling, the catalysts were crushed and screened to 20–40 mesh for using.

The evaluation of the catalyst was carried out in a fixed-bed tubular microreactor, equipped with a constant-flow pump to control the flow rate and a controlled heating system to maintain the temperature. The treated catalyst was packed between two quartz sands (40–60 mesh) and inserted into the reactor. The reaction was carried out under the following conditions: reaction temperature 448 K; reaction pressure 1 MPa; weight hourly space velocity (WHSV) at 30 h^{-1}. Samples of the inlet and effluent liquids from the reactor were analyzed with the bromine index analyzer every 30 min. The value of olefin conversion $(X) = [(n_o - n_i)/n_o] * 100$, where n_o is the initial content olefins and n_i is final content of olefins. Bromine Index is determined according to ASTMD 2710-92, which is a measure of milligrams of bromine consumed by 100 g of the sample under given conditions.

3. Results and discussion

3.1. Chemical analysis

The XRD patterns of USY and the modified USY zeolites obtained by treatment with different concentrations of citric acid are presented in Fig. 2.

Table 2 gives the Si/Al ratios, crystallinity and cell parameter (a_0) for treatments with citric acid. The global and framework Si/Al ratios were determined, respectively, by X-ray fluorescent (XRF) and XRD, the latter using the correlation established by Fichther-Schmittler et al. [15]:

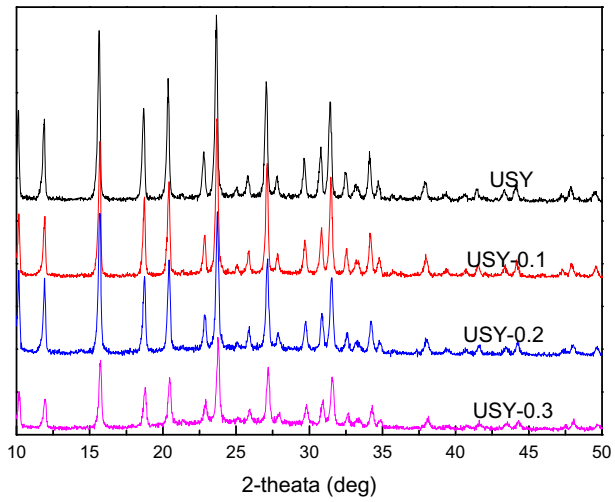

Fig. 2. XRD patterns of different samples.

Table 2
Characteristic of samples treated with citric acid.

	Sample			
	USY	USY-0.1	USY-0.2	USY-0.3
Framework Si/Al	2.43	3.62	6.39	9.11
Global Si/Al	1.78	1.95	2.31	2.54
Crystallinity	100%	83%	81%	56%
a_0 (nm)	2.92	2.79	2.65	2.59

$$\left(\frac{Si}{Al}\right)_{XRD} = \frac{192}{112.4 \times (a_0 - 2.4233)} - 1 \quad (3)$$

Where a_0 is the cell parameter in nm. The cell parameter precision is estimated to be 0.001 nm, leading to a relative precision for the ratio Si/Al of the order of 10% in the range studied. Crystallinity of the solids was also determined by XRD using the ratio of the sum of zeolite peaks to background with the USY starting material as reference.

The USY zeolite has been modified by hydrothermal treatment, which can result in the dealumination of the skeleton with total content of Al, Si and Na remaining unchanged [16]. However, it's dealuminum degree is rather limited and the non-framework aluminum formed during the steam treatment may affect the catalytic performance. Here the modification is a new effective method to treat USY zeolite with organic acid in the unbuffered system.

The crystallinity of the samples decreased with the increasing concentration of acid, which implying the crystal structure became faulty with the leaching of Al component to form mesopores [17]. The aluminum is removed from the zeolite crystal as a soluble aluminum complexes. Simultaneously, some extra framework silica fills the skeleton vacancies left by aluminum. Thus, the modification process is believed to result in framework reconstruction with the USY zeolite skeleton. There is no obvious peak in the modified samples (USY-0.1, USY-0.2 and USY-0.3), which implying the EFAL presented in the form of amorphous material.

3.2. N_2 adsorption analysis

The pore sized distributions of the USY parent and USY treated with different concentrations of citric acid using the BJH model to desorption branch of the isotherm was presented in Fig. 3. It can be found that there was a peak at 4 nm after modified by citric acid. A large amount of mesopores was generated with the modification of

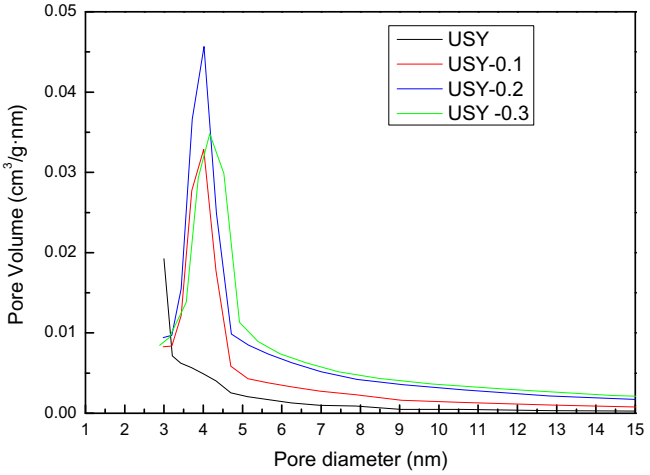

Fig. 3. Pore size distributions of different samples.

citric acid and the amount increased with the enhancement of concentration of the citric acid.

The isotherms of nitrogen adsorption (Fig. 4) on both USY-parent and the representative modified USY samples (USY-0.2) are similar to type IV. The hysteresis loop indicated the presence of mesopores with the capillary condensation of liquid nitrogen on its surfacel [18].

It has also been found that the relative pressure (P/P_0) of USY-0.2 at which the adsorption reaches the last plateau shifts to the right for a sample with larger pore diameter [19]. This characteristic relative pressure (P/P_0) is well known as the indicator used to qualitatively compare the pore dimensions of different samples and the higher value has a mesopore size.

It is demonstrated that the modification process of USY zeolite makes more development pore volume than the parent one, while the shape of the isotherm is not changed.

Table 3 presented the result of surface area and pore volumes for USY and USY-0.2. It can be found that the mesopore area and mesopore volume of the USY-0.2 became larger than that of the USY sample. It was also proved that the mesopores was generated during the modification process.

3.3. In situ FT-IR investigation

The FT-IR spectra of different samples were presented in Fig. 5. There is a sharp band due to stretching vibrations of OH groups

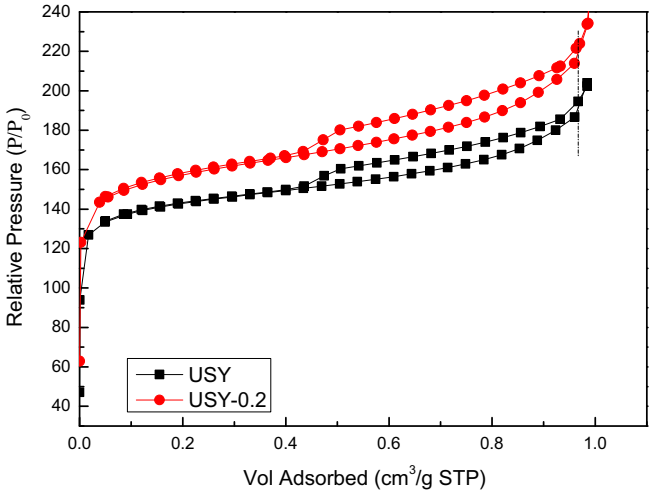

Fig. 4. The isotherms of USY-0.2 and USY parent.

Table 3
Textural properties of the investigated samples.

Samples	Surface area (m^2/g)	Mesopore area (m^2/g)	Pore volume (cm^3/g)	Mesopore volume (cm^3/g)
USY	480.66	38.14	0.158	0.034
USY-0.2	537.62	80.27	0.223	0.086

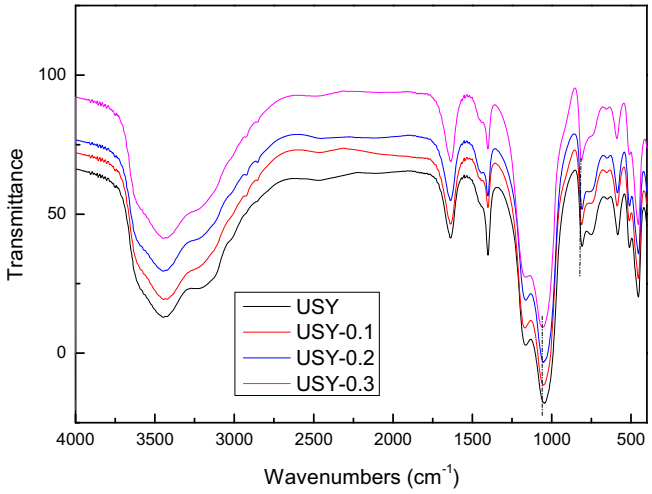

Fig. 5. FT-IR spectra of different samples.

which appeared in the wave number 3500 cm^{-1}. It is attributed hydroxyls in mesopore or large cages [20–21]. Additionally, the two bands at 1050 and 810 cm^{-1} shifted toward high wavenumbers with the increase of concentration of citric acid, implying a higher Si/Al ratio [22].

The adsorption of pyridine as well known indicator for acidic sites, was investigated by infrared spectroscopy. The IR spectra in the 1600–1400 cm^{-1} region are showed in Fig. 6. There are three sharp bands due to N–H stretching vibrations of pyridine. The strong band at 1490 cm^{-1} is due to the pyridine adsorbed on both Lewis (L) and Brønsted (B) acid sites [23], while bands at 1540 cm^{-1} and 1450 cm^{-1} are due to protonation of pyridine

Table 4
Acidic properties of different samples.

Sample	Total acid sites ($\times10^{-4}$ mol g^{-1})	Total L acid sites ($\times10^{-4}$ mol g^{-1})	Total B acid sites ($\times10^{-4}$ mol g^{-1})
USY	51.41	1.33	50.08
USY-0.1	49.68	13.11	36.57
USY-0.2	38.11	15.45	22.66
USY-0.3	36.47	20.33	16.14

molecule by Brønsted acid sites and pyridine adsorbed on Lewis acid sites, respectively [24–25].

The concentration of Lewis and Brønsted acid sites were calculated by the Lambert–Beer law, showed in Table 4. Of interesting is that the number of total acid sites decreases with the increasing of the concentrating of the citric acid solution, while the molar ratio of Si/Al has the opposite change trend. It can be assumed that the Al content determined the amount of the acidity sites [26].

PyAl complexes found on modified samples can be considered as being formed from skeletal three-coordination aluminum atoms [27]. It also can be found that the amount of Lewis acid increased with the concentration of the citric acid from Table 4. This phenomenon can be explained since the removal of aluminum requiring partial rearrangement of aluminosilicate framework may be formulated as follows [28]:

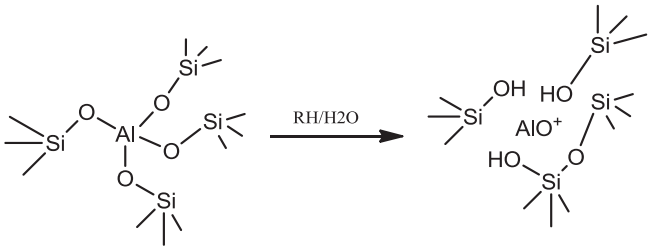

The Al removed from the framework of zeolite was existed as the form of AlO^+ species. The AlO^+ species can supply the Lewis acid sites in the zeolite. The positive charge sited on the extra framework AlO^+ was the main reason for the decrease in the number of acid sites and the increases in Lewis acid sites [29].

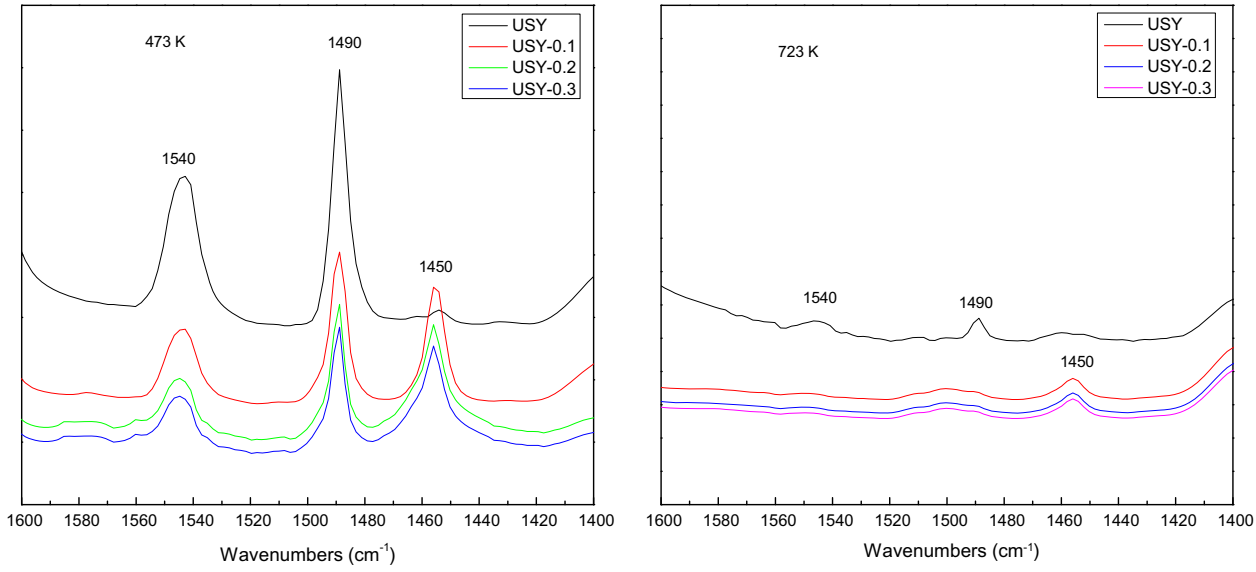

Fig. 6. Comparison of pyridine-IR spectra for different samples.

Aluminum atom concentrations per unit cell were calculated from the Si/Al ratios on the basis of 192 T atoms (Si or Al) per unit cell. The number of extra-framework Al per unit cell was then derived as the difference between the total number of aluminum atoms (measured by XRF) and the number of framework aluminum atoms (measured by XRD). The extra-framework Al (EFAL) concentration per unit cell can be calculated through this formula:

$$\mathrm{EFAL} = \frac{192}{b+1} - \frac{192}{c+1} \tag{4}$$

Where b is the global Si/Al and c is the framework Si/Al in Table 2. Calculated values of extra-framework Al concentration of per unit cell are illustrated in Table 5.

For zeolite, The composition is $c(SiO_2) + 1(AlO_{1.5})$ and the isomorphous substitution of one Al atom generates one B acid site [30]. The B acid sites can be determined by the equation:

$$F = \frac{1}{c \times 60 + 51} \tag{5}$$

Where c is the framework Si/Al, F is the B acid sites concentration. The results were presented in Table 5. Because the upper limit of acid amount is the aluminum content, the values were more than that in Table 4. This phenomenon confirmed that the data of acid sites was credible in Table 4.

By using the power law equation, it is possible to write formulas between the concentration of L acid sites and EFAL. The parameter of the follow equation can be found in Fig. 7. As showed in Fig. 7:

$$Y = -0.00193 + 1.9 \times 10^{-4} \times X - 2.37 \times 10^{-6} \times X^2 \tag{6}$$

Where Y is the concentration of L acid sites and X is the EFAL. Following consideration of the Eq. (4), the relationship between L acid sites concentration and Si/Al can be obtained.

$$Y = -0.00193 + 1.9 \times 10^{-4} \times \left(\frac{192}{b+1} - \frac{192}{c+1}\right) - 2.37 \times 10^{-6} \times \left(\frac{192}{b+1} - \frac{192}{c+1}\right)^2 \tag{7}$$

Table 5
The properties of extra framework aluminum.

	Sample			
	USY	USY-0.1	USY-0.2	USY-0.3
EFAL	13	24	34	35
Framework Al	56	42	26	19
B acid sites ($\times 10^{-4}$ mol g^{-1})*	50.81	37.29	23.02	16.73

* The values of B acid sites concentration were calculated through formula (5).

Herein, the property of acid sites can be calculated by the Si/Al ratio in zeolite.

3.4. Micro-activity test evaluation

The activity of different samples for removing trace olefins from aromatics was investigated in the laboratory, and the correlation between conversion of olefins and duration was presented in Fig. 8. Considering the conversion above 90%, the effective running time was 2.5 h, when the USY parent was used as catalyst. Of special is that the effective running time increased drastically after the USY was treated with citric acid solution. It is noted that the sample of USY-0.2 lasts for 6 h, about 2.4 times as long as that of the parent zeolite. It can be concluded that the citric acid treatment as an important method for prolonging the lifetime made the zeolite showing a great superiority over the parent sample.

It is well known that acidity is a critical factor affecting the performance of the catalyst for removing trace olefins from aromatics [31]. Experimentally, the lower acidity of B acid restrained the higher effective running time. The L acid sites were responsible for the improvement of the catalytic activity. It can be found that the framework Al of USY-0.3 was least in all samples, which implying that the structure of USY-0.3 had been destroyed. The running time of USY-0.3 was shorter than that of USY-0.2, although the amount of L acid sites in USY-0.3 had an advantage.

For comparison, the performance of MCM-41 zeolite which had rich mesopores in this structure was presented in Fig. 8. The beginning conversion was only 23.2% when the olefin was treated over MCM-41. It was suggested that the olefin removing reaction mainly occurred in micropores. Because of the reagent can diffuse easily in mesopores, the mesopores can work to reduce the deactivation.

Carbonaceous compounds (coke) blocked inside the pores or on the surface of zeolites are responsible for their deactivation during the various processes of refining and petrochemicals [32]. The deactivation of USY zeolite catalysts can be due to a limitation of access of the reactant to the active sites or a blockage of the access. The pore blockage appeared at high coke content was caused by coke molecules located on the outer surface of the crystallites [33]. It was the reason for the pronounced deactivation in Fig. 8.

Indeed, the strongest acid sites, hence the most active, are the first to be deactivated, resulting in a large deactivating effect on the coke molecules at low coke content [34]. From the Table 4, it can be seen that the USY has a large number of Brønsted acid sites which will cause pore blockage. After modification, the decrease of

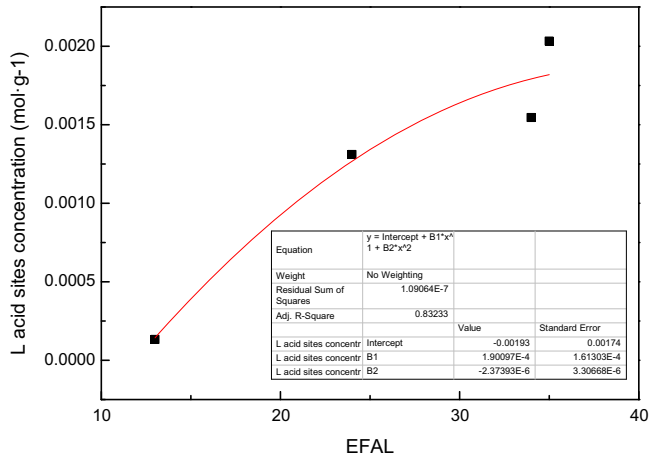

Fig. 7. The L acid sites concentration plotted against the extra framework Al.

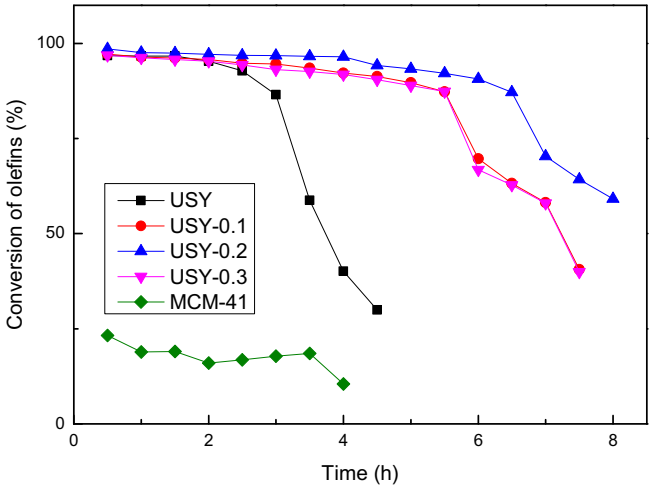

Fig. 8. Conversion of olefins of different samples in the laboratory.

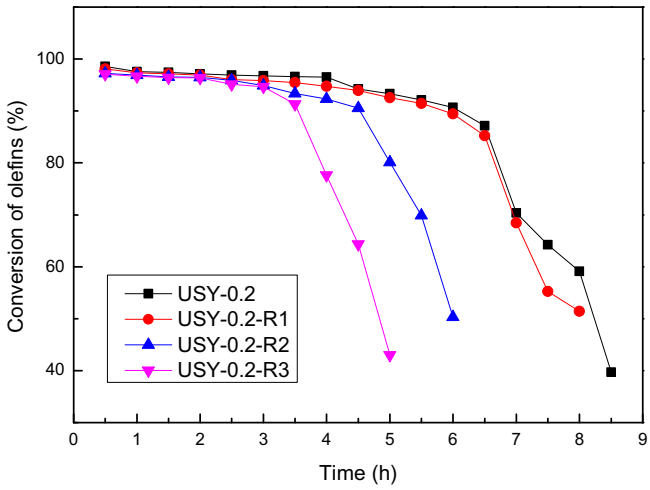

Fig. 9. Recycling study of USY-0.2 in removing trace olefins.

Table 6
The raw materials for studying of purifying process.

Component	Content W, %
1-Octene	4
Ethylbenzene	50
P-xylene	30
M-xylene	16

the deactivated ratio was due to the change of distribution of the acid sites. In addition, the mesopore pore generated during the acid treatment can diffuse out the coke before they cause pore blockage.

The reusability of the USY-0.2 was explored (Fig. 9). The experiment of regeneration was carried out through an oxidative treatment under air flow. The temperature employed was 823 K and the duration of the treatment was 6 h. The USY-0.2-Rn (n = 1, 2, 3) means the regenerated times of inactivating catalyst. Of significant was that the catalyst still remained 3.5 h when the conversion of olefins above 90% after three repeated experiments.

3.5. Study of the purifying process

In order to explore the process of the reaction between aromatics and olefins, the aromatics which had added the trace 1-octene was used as the raw materials. The components of the aromatics were showed in Table 6.

At the same condition (the reactor operating temperature was about 448 K, the reaction pressure was 1.0 MPa and the volume space velocity was 30 h^{-1}), the USY-0.2 was used for removing the olefins from this kind aromatics. The GC–MS analysis was conducted on the product from the reactor after 1 h. The result was presented in Fig. 10.

The Fig. 10(a) was the chromatogram of raw material. The Fig. 10(b) was the chromatogram of products treated by USY-0.2. The Fig. 10(c) was the chromatogram of products treated by USY. The Fig. 10(d) showed the mass spectrum of the main reaction products in the Fig. 10(b). It could be observed that the products mainly contained $C_{16}H_{26}$ from Fig. 10(d). Furthermore, it can be found that the 1-octene reacted with ethylbenzene and xylene to form $C_{16}H_{26}$ from the mass spectrum. It was confirmed that the mechanism of the olefins reacts with the aromatics was in accordance with the carbonium ion mechanism and the reaction is the alkylation reaction. The alkylation product can be also found in Fig. 10(c), when the model oil was treated by the USY zeolite. The trace olefin was removed from the aromatics through the alkylation reaction, whether the catalyst used was USY or USY-0.2. However, it had a longer lifetime when the aromatics was treated by the USY-0.2. Much L acid site in the USY-0.2 which can resist the coke formation was responsible for the enhancement of lifetime.

On the basis of that mechanism, the reaction mechanism between 1-octene and aromatics was illustrated in Fig. 11. The olefins molecule can be protonated by the B acid sites or L acid sites to a carbonium ion. For the enhancement of the running time was mainly caused by the L acid sites, the Fig. 11 only gave the processes activated by L acid sites.

The olefins molecule was protonated by L acid to a carbonium ion that generated, by electrophilic attack on the aromatic π-electrons, a mono or polyalkylbenzenium ion. The desorption process and the loss of the proton gave the alkylated aromatic and restored the L acid sites.

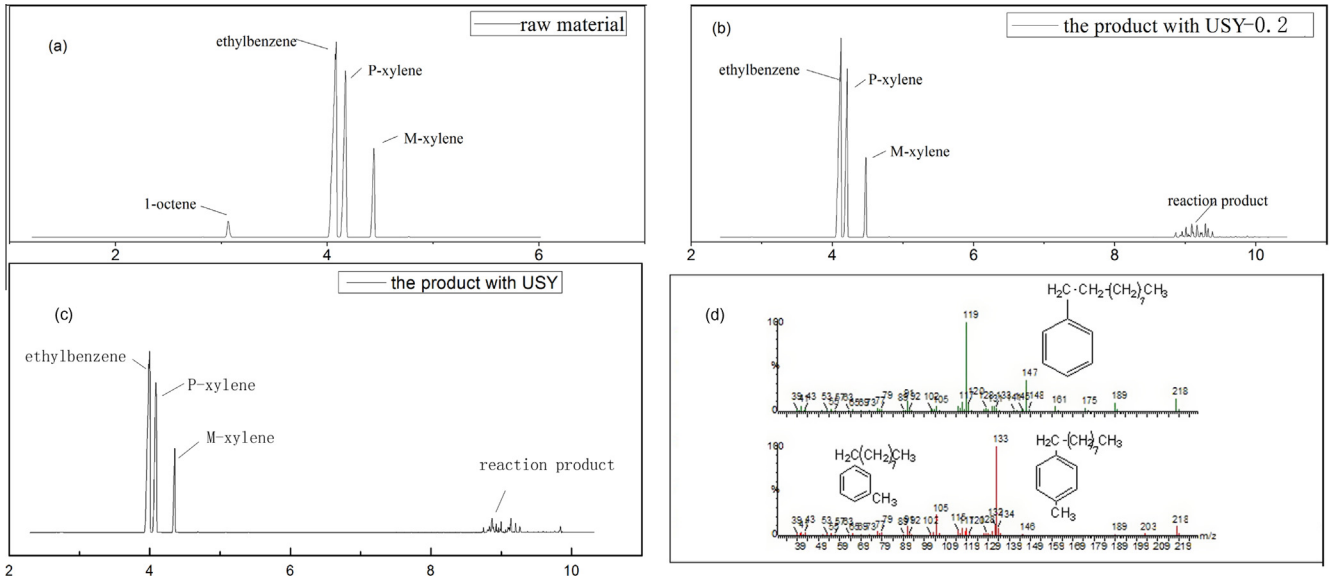

Fig. 10. The result of GC–MS analysis for different samples.

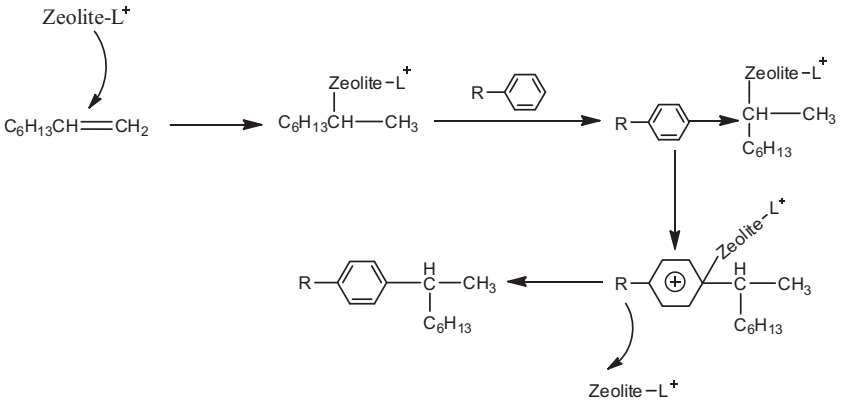

Fig. 11. The reaction mechanism between 1-octene and aromatics.

4. Conclusions

Dealumination of USY zeolite proceeds in a manner of citric acid treatment. The pore and acid properties of USY zeolite had been modified. Due to the process of extracting Al from the framework of USY, more mesopores was generated. In addition, the amount of B acid sites was decreased, while the amount of L acid sites was increased.

An approach to the quantification of the property of acid sites has been possible. The relation between acid properties of zeolite and the ratio of Si/Al was determined. The L acid site concentration can be obtained from the EFAL by the formula in this paper.

The modified USY is a promising catalyst for removing trace olefins from the aromatics with a high lifetime than the parent USY. The reduction of the B acid site and the enhancement of the L acid in the samples was contribute to the high activity. Much L acid site can contribute the longer lifetime of catalysts because of its resistance for coke formation. The mesopores which was generated during the modification process could reduce the deactivation by increasing in diffusion through increased pore openings.

Acknowledgment

The authors gratefully acknowledge the financial support by the Sinopec Zhenhai Refining and Chemical Company through the applied research program.

References

[1] S.H. Brown, J.R. Waldecker, M. Lourvanij, Process for reducing bromine index of hydrocarbon feedstocks, U.S. Patent 7,744,750,2005.
[2] H.B. Stephen, E.H. Terry, P.W. Arthur, Decreasing BI-reactive contaminants, U.S. Patent 6,368,496 B1, 2002.
[3] J.N. Luan, G.L. Li, L. Shi, Ind. Eng. Chem. Res. 50 (12) (2011) 7150–7154.
[4] X. Pu, N.W. Liu, Z.H. Jiang, L. Shi, Ind. Eng. Chem. Res. 51 (43) (2012) 13891–13896.
[5] G.L. Li, J.N. Luan, X.S. Zeng, L. Shi, Ind. Eng. Chem. Res. 50 (11) (2011) 6646–6649.
[6] T. Montanari, E. Finocchio, G. Busca, J. Phys. Chem. 115 (2011) 937–943.
[7] R.H. Abudawood, F.M. Alotaibi, A.A. Garforth, Ind. Eng. Chem. Res. 50 (2011) 9918–9924.
[8] Clarence D. Chang, N.J. Princeton, Dealuminization of aluminosilicates, U.S. Patent 4273753, 1981.
[9] J. Klinowski, J.M. Thomas, M.W. Anderson, C.A. Fyfe, G.C. Gobbi, Zeolite 3 (1) (1983) 5–7.
[10] D.C. Clarence, T.W.C. Cynthia, N.M. Joseph, F.B. Robert, R.C. Bruce, J. Am. Chem. Soc. 106 (1984) 8143–8146.
[11] X.M. Liu, Z.F. Yan, Catal. Today 68 (2001) 145–154.
[12] Z.M. Yan, D. Ma, J.Q. Zhuang, et al., J. Mol. Catal. A: Chem. 194 (2003) 153–167.
[13] M. Guisnet, P. Ayrault, J. Datka, Pol. J. Chem. 71 (1997) 1455–1461.
[14] M. Guisnet, P. Ayrault, C. Countanceau, M.F. Alvarez, J. Datka, J. Chem. Soc., Faraday Trans. 93 (1997) 1661–1665.
[15] H. Fichtner-Schmittler, U. Lohse, G. Engelhardt, V. Patzelová, Crystal Res. Technol. 19 (1984) K1.
[16] M. Kojima, F. Lefebvre, Y.B. Taarit, Zeolite 12 (1992) 724–727.
[17] S. Lopez-Orozco, A. Inayat, A. Schwab, T. Selvam, W. Schwieger, Adv. Mater. 23 (2011) 2602–2615.
[18] M. Gautier, F. Muller, L. Le Forestier, J.M. Beny, R. Guegan, Appl. Clay Sci. 49 (2010) 247–254.
[19] J.S. Beck, J. Am. Chem. Soc. 114 (1992) 10834–10843.
[20] H.J. Rauscher, D. Michel, H. Pfeifer, J. Mol. Catal. 12 (1981) 159–171.
[21] X. Yang, L. Zhou, C. Chen, X. Li, J. Xu, Mater. Lett. 63 (2009) 1754–1756.
[22] B.A. Holmberg, H. Wang, Y. Yan, Micropor. Mesopor. Mater. 74 (2004) 189–198.
[23] P. Kalita, N.M. Gupta, R. Kumar, J. Catal. 245 (2007) 338–347.
[24] V.T. Hoang, L.H. Qing, U. Adrian, E. Mladen, T.O. Do, K. Serge, Micropor. Mesopor. Mater. 92 (2006) 117–128.
[25] S.V. Awate, S.B. Waghmode, M.S. Agashe, Catal. Commun. 5 (2004) 407–411.
[26] A. Corma, F.V. Melo, D.J. Rawlence, Zeolites 10 (1990) 690–694.
[27] A.K. Ghosh, G. Curthoys, Faraday Trans. 79 (1983) 805–813.
[28] P.N. Aukett, S. Cartlidge, I.J.F. Poplett, Zeolites 10 (1986) 169–174.
[29] L. Antonio, de, P. Canizares, A. Duran, A. Carrero, Appl. Catal. A: Gen. 154 (1997) 221–240.
[30] K. Naonobu, M. Tetsuo, A.B. Hosne, N. Norihiro, N. Miki, J. Phys. Chem. B 104 (2000) 5511–5518.
[31] X. Pu, L. Shi, Catal. Today 212 (2013) 115–119.
[32] K. Moljord, P. Magnoux, M. Guisnet, Catal. Lett. 28 (1994) 53–59.
[33] M. Guisnet, P. Magnoux, Catal. Today 36 (1997) 477–483.
[34] M. Guisnet, P. Magnoux, Appl. Catal. 54 (1984) 1–27.